Microbend Point and Distributed Fiber Optic Corrosion Sensing

Matej Njegovec, Vedran Budinski, Boris Macuh, and Denis Đonlagić, *Member, IEEE*

***Abstract*— Corrosion-induced optical fiber microbending is demonstrated within this article as an efficient method for the design of sensors for the detection and localization of corrosion events on monitored metal surfaces. The proposed sensors were demonstrated in a single point and fully distributed configurations while applied successfully on bare metal surfaces and underneath corrosion-protective coatings. The intrinsic simplicity in the design and manufacturing of the proposed sensors, reliable corrosion detection, and corrosion localization are the main attributes of the proposed microbend corrosion sensing concept.**

***Index Terms*— Corrosion sensor, corrosion under the coating, distributed corrosion sensor, fiber optic sensor, microbend optical sensor.**

I. Introduction

THE presence and onset of corrosion processes of metallic objects impacts and degrades maritime, aeronautical, civil, and other structures significantly. Corrosion leads to degradation of structure performance, safety issues, and high maintenance costs. Online monitoring and early detection of corrosion processes could thus increase the long-term performance of different structures, mitigate safety issues, and reduce maintenance costs.

Standard corrosion detection methods include ultrasonic testing [1], radiographic testing [2], magnetic flux leakage [3], various electrochemical methods (linear polarization resistance, galvanic monitoring, and biological monitoring) [4], [5], and electrical methods (electrical resistance measurements) [6], while those methods are well established and standardized, they can be utilized mainly during scheduled maintenance procedures when the metallic structure under test is not in regular operation (usually, a trained person is required to scan the surface using the selected method). Furthermore, such methods often do not allow automatic location identification and real-time monitoring of the corrosion on larger metallic surfaces during operation in field applications. Developing suitable corrosion sensors that would enable online monitoring, would, thus, be of high interest in managing and monitoring a broad variety of metal structures and applications.

While some of the abovementioned inspection methods can be utilized in online measurements, they usually provide localized information and are susceptible to, or restricted by, environmental impacts. Fiber optic corrosion sensors offer an attractive alternative for corrosion sensing and detection, as they are intrinsically corrosion-resistant, fully dielectric, and immune to electromagnetic interference. Furthermore, optical fibers have sufficiently small diameters (typically 125 μm) to allow their unobtrusive mounting onto the monitored surfaces and can provide the possibility for fully distributed sensing. Different fiber sensor designs for corrosion detection were proposed in the past [7], [8], [9], [10]. Several sensor designs were reported, which utilize a sacrificial metallic layer applied into an optical fiber [11], [12], [13], [14], [15]. A section of fiber cladding is removed and replaced by the metallic layer in these designs. During the corrosion process, the metallic layer is removed, exposing the fiber's core to the surrounding environment. This causes a change of the fiber's effective refractive index at the exposed region, resulting in a change in the sensor's transmission/reflection spectrum [11] or change in transmitted optical power [16]. While the corrosion process of the applied metallic film can be detected reliably, this type of sensor does not detect corrosion's presence directly on the target surface. Furthermore, the manufacturing and deposition of the metallic layer is often not straightforward and requires proper sample preparation. Another approach for detecting corrosion is based on the measurement of change in the strain of a metallic surface during the corrosion process. Metal surfaces expand during the corrosion process, and this can be detected by measuring the surface strain. For example, corrosion sensors based on fiber Bragg gratings (FBGs) [17], [18], [19] or macro-bend-induced losses [20] were demonstrated successfully in the past. The challenge herein is a proper fixture of the sensor on the metal surface to allow reliable strain transfer while providing unobstructed exposure of the sensing area to a corrosive environment (adhesive can prevent or slow down the corrosion process). Most sensors of this type are designed for single-point measurements and can be, in the best case, extended to quasi-distributed (multipoint) sensing configurations (FBGs) [21]. Fully distributed strain sensing might also be applied for distributed corrosion sensing. These systems are usually based on Brillouin optical time-domain analysis [22], [23], [24] or optical frequency-domain reflectometry [25], [26], which rely on the measurement

Manuscript received 25 April 2022; revised 8 July 2022; accepted 13 August 2022. Date of publication 2 September 2022; date of current version 22 September 2022. This work was supported by the Office of Naval Research (US) under Grant 12827129. The Associate Editor coordinating the review process was Yuya Koyama. *(Corresponding author: Matej Njegovec.)*

The authors are with the Faculty of Electrical Engineering and Computer Science, University of Maribor, 2000 Maribor, Slovenia (e-mail: matej.njegovec@um.si).

Digital Object Identifier 10.1109/TIM.2022.3203450

of strain along the single-mode fiber attached to the target surface. While these methods offer good spatial resolution (several millimeters), they require complex and expensive optoelectronic and electronic signal processing and often depend on challenging installation procedures (for example, winding of the fiber around the target object [22], [23], [24], [25]). Furthermore, different and time-dependent strain profiles are common in normal structure operation. These must be distinguished clearly from the strain profiles caused by the onset of corrosion, which might further limit strain-based corrosion sensing capability.

This article presents an alternative fiber-optic corrosion sensor based on the appearance of optical losses in multimode (MM) fibers caused by corrosion-process-induced fiber microbending. The proposed sensor provides simple, unobtrusive, and straightforward installation, while it relies on uncomplex signal interrogation, even in a fully distributed configuration. Special attention was devoted to detect the corrosion under the protective coatings.

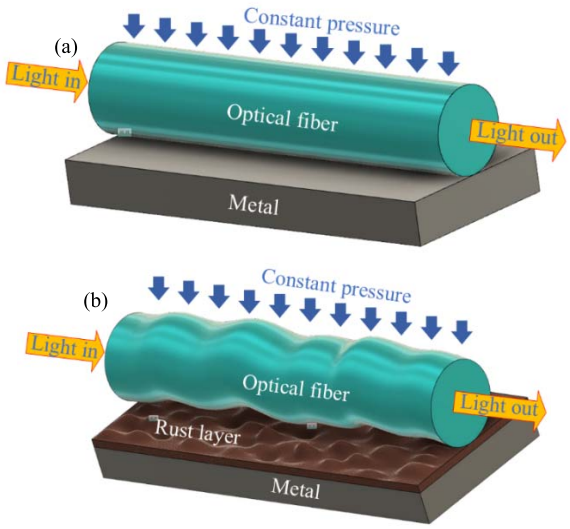

Fig. 1. (a) Fiber depressed on a smooth metal surface. (b) Fiber microbend perturbations due to the random expansion of rust.

II. Sensor Design

A. Basic Principle of Operation

The corrosion of metallic surfaces causes local growth and expansion of a surface's material volume. This local expansion is nonuniform and often associated with local rust flakes' formation, which converts the initially smooth metal plane into a microscopically rough and uneven surface. In anti-corrosion-protected surfaces, the surface transformation often occurs under a protective polymer layer(s) (coatings). When a suitable optical fiber is fixed or depressed against the observed metal surface (by a mechanical fixture, adhesive or even protective coating as described in the following chapters) [see Fig. 1(a)], the corrosion-initiated surface expansion creates randomly distributed pressure onto the fiber due to the expansive force of rusting (oxide jacking). This perturbs the fiber in a direction perpendicular to the fiber axis, which results in the appearance of fiber microperturbations [see Fig. 1(b)].

The fiber transmission losses depend strongly on these fiber off-axis microperturbations, so relatively simple and effective microbend corrosion sensors can be formed.

Within this investigation, two variants of microbend corrosion sensors were investigated:

1) microbend corrosion sensors based on a randomly perturbed optical fiber;
2) microbend corrosion sensors based on a periodically perturbed optical fiber.

B. Microbend Corrosion Sensors Based on a Randomly Perturbed Optical Fiber

In this sensor configuration, the optical fiber is depressed uniformly against an observed and initially smooth and uncorroded metal surface, as shown in Fig. 1(a). In case of the appearance of corrosion on the metal surface, the local expansion of the surface displaces the fiber randomly along its length in a vertical direction, as shown in Fig. 1(b). This causes transmission loss modulation, which depends on the perturbed fiber's length and the amplitude of the corrosion-induced perturbations.

However, this relatively straightforward approach suffers from a weak amplitude of fiber perturbations that can be achieved in a practical system and, thus, requires sufficiently microbend-sensitive fibers. Initial tests conducted using telecom MM fibers showed too low sensitivity for their use in most practical corrosion sensing applications. While the amplitude of the microbend perturbation depends on the metal/surface properties, the type of the corrosion process, the thickness of the protective layer, and the protective layer's elastic properties, these effects combined have a substantially weaker impact on the sensitivity of the proposed sensor than the properties of the sensing fiber. The microbend sensitivity of an MM fiber is governed primarily by the separation of the highest order modes in the phase constant space. A power coupling coefficient h_{xy} among two modes in the randomly perturbed fiber can be expressed as [27]

$$h_{xy} = C\frac{1}{\Delta\beta^4}F(\Delta\beta) \tag{1}$$

where $\Delta\beta$ represents the phase constant difference between two coupled modes, and C is a constant dependent on the fiber's geometry and coupled modes field distributions, while $F(\Delta\beta)$ represents the power spectrum of the fiber curvature function taken at $\Delta\beta$.

For a step-index profile fiber, $\Delta\beta$ can be expressed further as [28]

$$\Delta\beta = \frac{2}{a}\sqrt{\Delta}\frac{m}{M} = \frac{\sqrt{2}\cdot \mathrm{NA}}{na}\frac{m}{M} \tag{2}$$

where a is a core radius, NA is a numerical aperture, n is the core refractive index, m is the mode order, and M is the highest order mode number. Since the power loss occurs by means of optical power leakage from the highest order modes to the continuum of cladding modes, the coupling between the highest order modes is of the main importance for the

microbend loss [28], i.e., $m = M$. By inserting (2) in (1) and setting $m = M$, we obtain

$$h_{xy} = C_{xy}\frac{1}{4}\left(\frac{na}{\mathrm{NA}}\right)^4 F(\Delta\beta). \tag{3}$$

To maximize the fiber's sensitivity to random bending perturbations, the core radius shall thus be maximized, while the NA shall be reduced. Both effects have a strong (highly nonlinear) effect on the microbend sensitivity of the fiber, as indicated by (3). Furthermore, the fiber's primary coating acts as a mechanical buffer layer, which can reduce sensitivity to microbend losses significantly. While shorter sections of the fiber might be stripped (coating removed), this is not practical for most field applications. In microbend applications, thinner and harder primary coatings are, thus, preferred over double-layer acrylate telecom coatings applied to standard telecom fibers. As the high microbend sensitivity to the microbending is generally an undesirable property of an optical fiber, the commercial availability of fibers with a large core, low NA, and thin and hard coatings is very limited. Among the exceptions are fibers designed for the production of high-power fiber laser pump combiners, where low NA and large core fibers are required to provide efficient coupling of multiple pumps into a single double-clad fiber. An example of such a fiber is AFM105/125/145 (Molex/Fiberguide) with a core diameter of 105 μm, NA = 0.12, the fiber diameter of 125 μm, and thin polyimide coating (total outer diameter of 145 μm). After an initial investigation of different commercially available fibers, this fiber was selected as the preferential fiber for the design of all microbend sensors used within this investigation.

The simplest form of the proposed microbend corrosion sensor is, thus, reduced to an appropriate fiber selection and fixing of the same fiber to the monitored surface to allow for the transfer of corrosion-induced surface microperturbations (oxide jacking) into vertical microdisplacements of the fiber. We investigated two different systems for fixing the fiber onto the observed metal surface: Firstly, a sensor setup with an additional element for mechanical depression of the fiber against the surface and secondly, direct incorporation of a fiber under the polymer anti-corrosion protective layer. Both versions of sensors are presented schematically in Fig. 2(a) and (b).

The system for mechanical depression of fiber against the surface [see Fig. 2(a)] consisted of a miniature spring stainless steel rod with cross-sectional dimensions 1 × 1.5 mm and a length of about 35 mm. The rod was prolonged into T-shaped extensions on each side, which were used to fix the rod onto the observed surface by M4 screws. Between the rod and the screws, we inserted a piece of 1-mm-thick rubber buffer, which allowed for more precise tightening of the steel rod without damaging/cracking the fiber. The bottom side of the rod was polished, and the sensing optical fiber was depressed between the sample metal surface and the spring steel rod. Force of depression was measured indirectly through the observation of transmission losses during mounting of the sensor. Screws were incrementally tightened till the transmission losses increased by 20%.

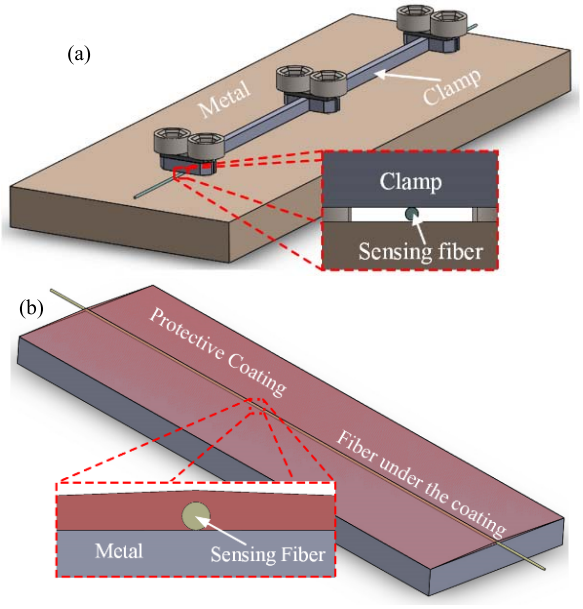

Fig. 2. (a) Sensor based on a mechanical fixture of the sensing fiber. (b) Direct mounting of the fiber under the protective polymer coating.

The second design approach omitted the mechanical fixture for fiber depression against the observed surface and was replaced by an anti-corrosion protective coating. In this case, the protective coating provides the function of depressing (fixing) the sensing fiber against the observed surface [see Fig. 2(b)]. Any special mechanical fixture for fixing the fiber against the observed metal surfaces is, thus, not necessary. The preparation of a random perturbation microbend corrosion sensor is, thus, reduced to the positioning of the fiber onto the observed metal surface, followed by the application and curing of the anticorrosion protective coating

C. Microbend Corrosion Sensors Based on a Periodically Perturbed Optical Fiber

While losses within a randomly perturbed fiber depend primarily on its core diameter and NA (3), they can be increased additionally if the fiber is perturbed periodically with a period that promotes the mode coupling, i.e., by maximizing $F(\Delta\beta)$ in (1). Since the power is lost from the fiber through the coupling of the highest order modes with a continuum of cladding modes [$m = M$ in (2)], critical perturbation period Λ_c, which maximizes $F(\Delta\beta)$ in (1), can be expressed as [28]

$$\Lambda_c = \frac{\sqrt{2}\pi a n_0}{\mathrm{NA}}. \tag{4}$$

For the same optical fiber as used in the case of the microbend sensor with random perturbations (AFM105/125/145), we obtain $\Lambda_c = 2.8$ mm. Periodic fixing of an optical fiber to the metal surface with the period Λ_c shall, thus, enhance the sensor's sensitivity to the corrosion process.

Several possible designs were investigated and tested of periodic fiber deformation structures. This included the investigation of mechanical gratings, photolithography-created polymer periodic fixtures, and other methods. Among the tested approaches, the most effective design was obtained by

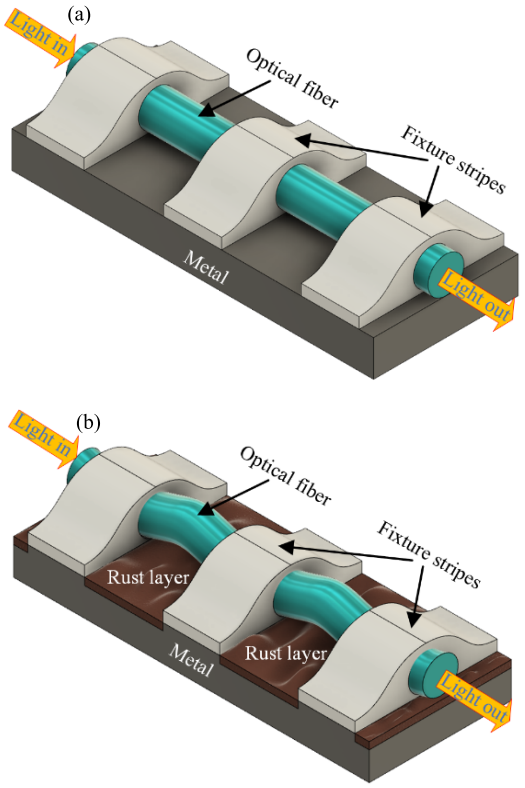

Fig. 3. Fiber fixed with periodic stripes. (a) Rust-free metal surface. (b) Corroded metal surface.

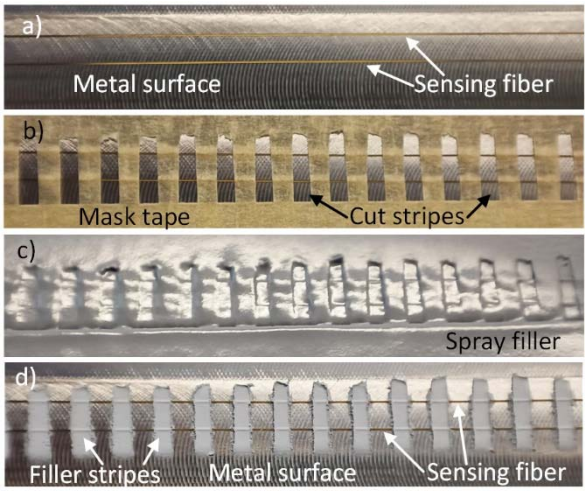

Fig. 4. Periodic sensor manufacturing process. (a) Fiber positioned on the metal surface. (b) Masking tape stencil positioned on top of the fiber. (c) Application of the spray filler. (d) Removal of masking tape stencil.

applying periodic stripes (see Fig. 3) created by a simple mask (stencil) and spray filler primer.

The manufacturing process is depicted in Fig. 4 and includes a few steps: initially, masking tape is cut out periodically to form an adhesive stencil. The fiber is then positioned over the desired surface [see Fig. 4(a)] and fixed by the cut mask tape [see Fig. 4(b)]. Spray filler (spray primer) is then applied over the stencil in three layers [see Fig. 4(c)]. After semi-curing

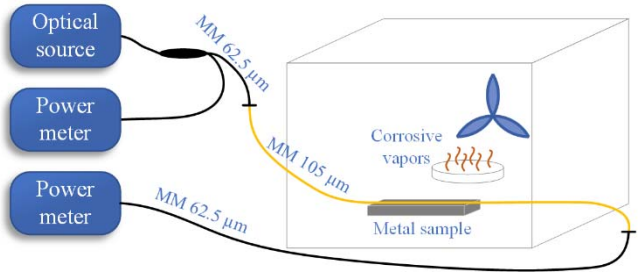

Fig. 5. Test setup for the corrosion sensors.

the filler, the stencil is removed, and the spray filler is left to cure fully [see Fig. 4(d)].

The presented manufacturing process is convenient, as the adhesive stencil holds the fiber firmly over the entire sensing length and thus allows for the installation of the sensor on uneven (curved) or more complexly shaped surfaces. Periodic stripes are also thin and can, additionally, be covered by a protective coating, thus allowing corrosion monitoring under the protective layer.

D. Distributed Sensor Designs

Microbend sensor designs using random fiber perturbations under protective coating and the stencil/spray-filler approach further covered by protective coating were applied to samples with long lengths to demonstrate the distributed sensing capability of the proposed sensor concepts as described further in Section III.

III. Experimental Results and Analysis

A. Experimental Setup for the Accelerated Corrosion Tests of Short/Point Sensors

All types of tested sensors were manufactured on metal tests samples with dimensions of 30 × 60 × 4 mm ($W \times L \times H$) made of S235JR + C steel. The surface of each sample was flattened (faced) using computer numeric control (CNC) milling. Samples were then cleaned thoroughly to remove any debris from the milling process and to eliminate the residues of the cooling fluid. The sensing fibers were attached to the surfaces of the prepared samples in accordance with procedures described in Section II.

To accelerate the corrosion process and measure the transmission losses, we prepared a test bench (see Fig. 5) made of an optical measurement setup and a test chamber. The test chamber comprised an airtight container filled with corrosive vapors formed by a 10% hydrochloric (HCl) acid solution in deionized water. HCl is highly oxidizing for most metals [29], [30], and initial tests showed fast penetration of the HCl vapors through the protective coatings. The corrosive vapors were distributed evenly around the chamber using a fan and natural evaporation. The metal samples (sensors) were inserted into the test chamber, while the transmission loss (microbend loss) at the sample/sensor was observed using the optical setup shown in Fig. 5.

The optical setup comprised a broadband optical source coupled into a standard telecom MM fiber with a core diameter of 62.5 μm (this mitigated the bend losses in the region

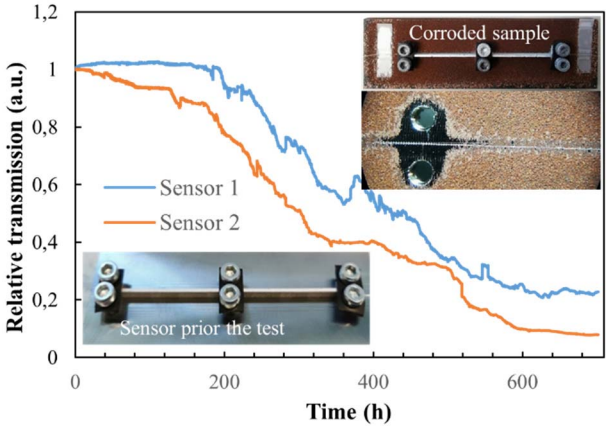

Fig. 6. Relative transmission of two fibers fixed with a mechanical fixture during exposure to corrosive vapors.

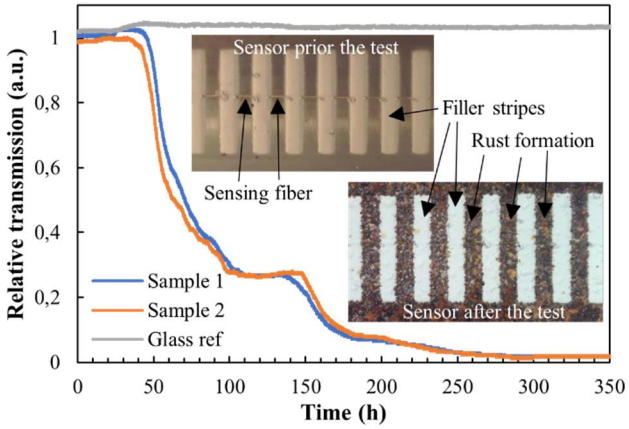

Fig. 7. Response of the two sensors based on periodic microbend and a reference sample.

between the interrogation system and the sensor). The fiber was then split using an MM optical coupler, where one branch was connected to the optical power meter and the other to the sensing MM fiber. Part of the sensing fiber was fixed onto the metal surface to form a sensor section (as already described in Sections II-A and II-B), and the end of the sensing fiber was connected to another section of standard MM fiber, which was further connected to the second optical power meter. The optical power meters were connected to a computer, running an application that divided both optical powers (i.e., normalized power in the sensor branch) to exclude variations in the optical power of the source. Several samples within the same chamber were tested simultaneously over longer periods of time. To assure that the measured transmission losses are induced by a corrosion process (and not by protective coating swelling or other deformations), we initially included a reference sensor made on a silica glass substrate, which did not change the properties under exposure to the corrosive vapors. We initiated the measurement process and recording several hours before introducing corrosive vapors to obtain reliable data on initial (reference) losses and ensure that coatings are fully dry and that the clamping force is constant. Initial losses were also used for the normalization of results.

B. Testing of Uncoated Sensors

The initial tests were performed with sensors mounted on uncoated metal samples. The first series of tests included sensor designs that utilized random perturbations using mechanical fixtures of the fiber to the metal surface (as described in Section II-A). Two sensors' optical transmission losses were observed over a period of about 700 h. The sensors were exposed initially to an atmosphere composed of ambient air for about 24 h, and afterward, a 10% solution of HCl was introduced into the test chamber in a separate container to provide a corrosive vapor atmosphere. During the first 180 h of the test, the sensors showed a limited response, but afterward, the relative transmitted optical power started to decrease nearly monotonically (see Fig. 6).

After 600 h of testing, the output power stabilized at about 10%–20% of the initial power, indicating a total loss increase caused by the corrosion process of about 8–10 dB. Comparison of the test samples before and after the test is shown in Fig. 6.

From the inspection of the sample after the test, we can observe that the sample did not corrode equally under the mechanical fixture and the rest of the sample. The mechanical fixture prevented the corrosive vapors' circulation into the vicinity of the fiber, and the response of the sensor was, thus, relatively slow. These tests were repeated several times, and Fig. 6 represents a typical response obtained during this type of test.

Further tests included corrosion sensors based on a periodic perturbation structure (Section II-C). Three sensors were prepared, where two were made on metal samples and one was made on a glass substrate. The sensor on the glass substrate served as a reference to verify possible impacts of the corrosive vapors on the periodic stripes (primer spray filler) and, consequently, on the sensor's behavior. The sensors were inserted into the test chamber and connected to the interrogation unit. Relative optical transmission over time was observed, and results are presented in Fig. 7.

The sensors were initially exposed to an atmosphere composed of ambient air for about 48 h; afterward, corrosive vapors were introduced into the chamber. Soon after corrosive vapors were introduced into the chamber, we observed a limited increase in transmitted optical power. Since it also happened on the reference glass substrate, we assume that spray filler slightly relaxed after exposure to highly chlorine reach environment. A rapid decrease in the sensor's transmission can be seen in Fig. 7 during the first 48 h after the introduction of the corrosive vapors, while the optical power stabilized fully after about 300 h. The two tested sensors had a nearly identical response and provided a deep modulation, with the final transmission of less than 1% of the initial value (20-dB loss modulation). The reference sensor transmission remained intact during the test duration, confirming that the change in the transmission is corrosion rather than adhesive/spray filler related. Visual inspection of the samples before and after the test shows the clear difference and rust formation around the exposed parts of the fiber (see Fig. 7). Between 100 and 150 h of the test, there were almost no visible changes during the

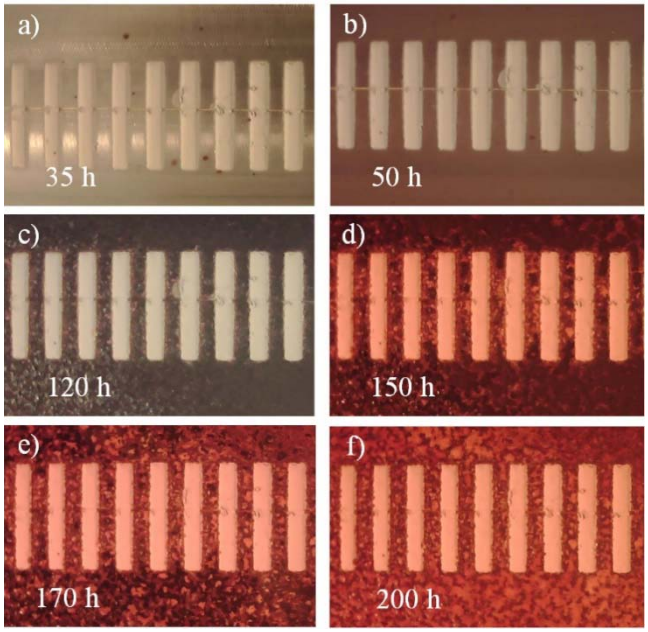

Fig. 8. Corrosion after (a) 35 h (clean sample), (b) 50 h (signs of fine rust), (c) 120 h (black rust), (d) 150 h (signs of brown rust), (e) 170 h (progression of brown rust), and (f) 200 h (brown rust).

corrosion process, and during this time, transmitted optical power remained constant.

There is also a step-like change in the loss curve slope at about 170 h, which can be observed for both sensors. This response of the sensors was most likely caused by different types of corrosion processes that form on the metal surface [see Fig. 8(a)]. Initially, fine black rust was formed on the surface [see Fig. 8(b)–(d)], but after about 170 h, we observed the formation of brown rust with larger rust flakes [see Fig. 8(e) and (f)].

According to this observation, the sensor could perhaps provide an opportunity for observing the type of rust formation; however, a more detailed investigation will be conducted to confirm this possibility.

C. Corrosion Detection Under the Protective Coating

To demonstrate the concept and operation of random and periodic microbend perturbation sensors under protective coating, we prepared a single metal sample (strip) 6 cm long, containing random and periodic microbend sensor configurations. Two samples of each sensor type (four sensors in total) were applied to the test metal sample (see Fig. 9). Both types of sensors were made on the same sample to assure that the corrosion rate was about equal across all sensors, which provided the possibility for a straightforward comparison of the results.

During the initial test, the metal strip sample was coated with several layers of the translucent general-purpose coating. While the translucent coating is not an efficient corrosion-protective coating, it allowed for visual observation of the metal surface and the fiber (see Fig. 9) under the coating before and after the test. Before the accelerated corrosion test, we measured the coating thickness using a laser scanning 3-D

Fig. 9. Section of a metal sample containing two periodic and two randomly perturbed sensors. The sample is coated using a transparent coating.

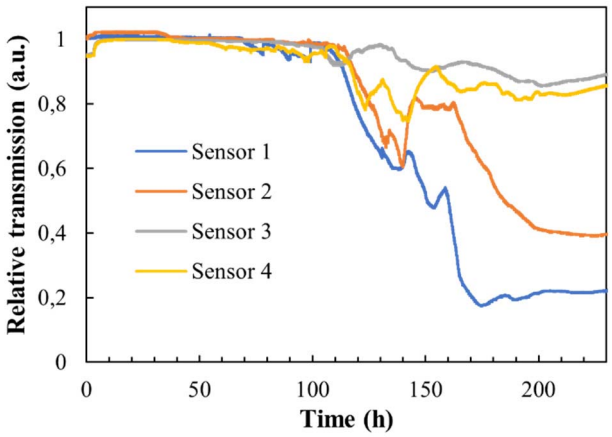

Fig. 10. Results from random and periodic perturbation corrosion sensors on the same metal sample.

microscope (OLS5100, Olympus), which showed the coating thickness of approximately 35 μm (the precise refractive index of the coating is not known; thus, the obtained thickness is only approximate).

The prepared sample was then inserted into the test chamber and exposed to corrosive vapors after the initial period of 4 h. The responses presented in Fig. 10 show that all sensors responded almost simultaneously after 110 h of exposure.

There is a clear difference in the sensitivity between the periodic and randomly perturbed sensors. Forcing the fiber into periodic microbending under the protective coating using a periodically applied hard spray filler caused a decrease in the relative transmission of over 50%, while the relative transmission of the randomly perturbed sensor decreased by only about 10% (see Fig. 10).

As will be further presented in the next chapter, periodic stripes offer better and more even fiber adhesion, especially on uneven surfaces. Masking tape with cut strips provides uniform fiber pressure against the target surface over the entire sensing length. This is much harder to achieve with direct bonding of the fiber to the metal surface, since any unevenness can decrease the bonding pressure or even separate the fiber from the target surface. Visual inspection of the samples allows the inspection of the formation of the corrosion under the coating (see Fig. 9).

The surface height change of the metal sample was measured on a 1200-μm-long section under the coating prior to the test and was approximately 1 μm (see Fig. 11), while, after the test, it exceeded 5 μm. Over time, random growth of

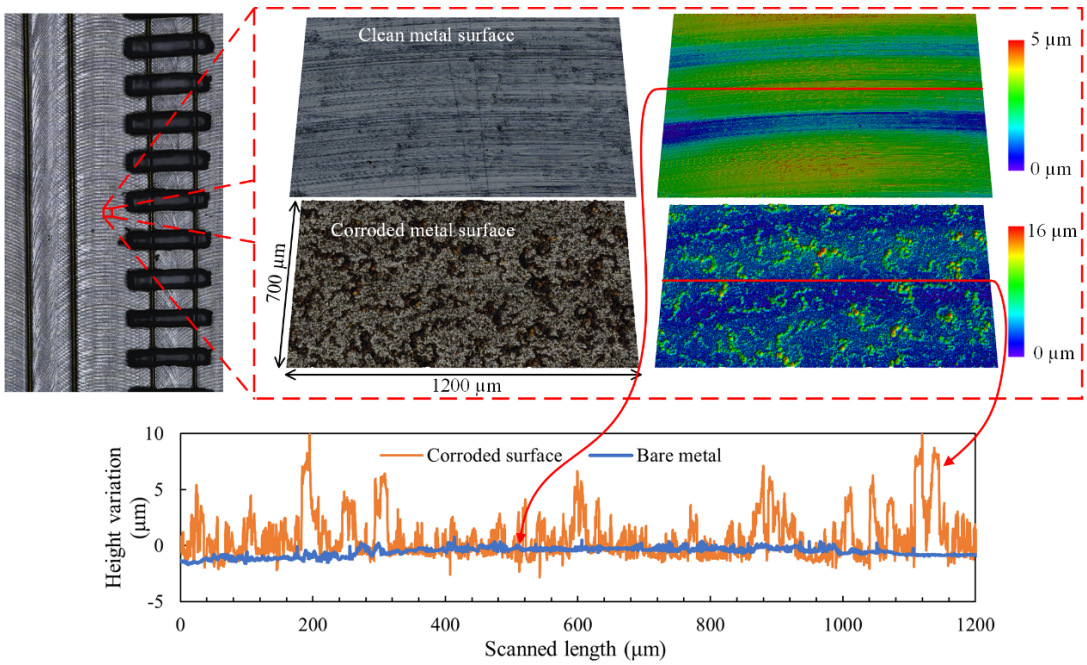

Fig. 11. 3-D scanned section of the metal sample before and after the accelerated corrosion test. The red line marks the location of the surface height variation measurement.

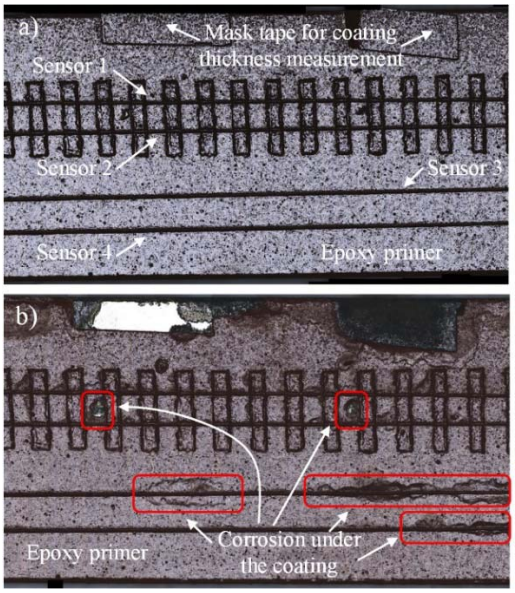

Fig. 12. (a) Test sample coated with epoxy primer prior to the test. (b) Test sample after the test. The red outlines mark the visible signs of corrosion under the coating.

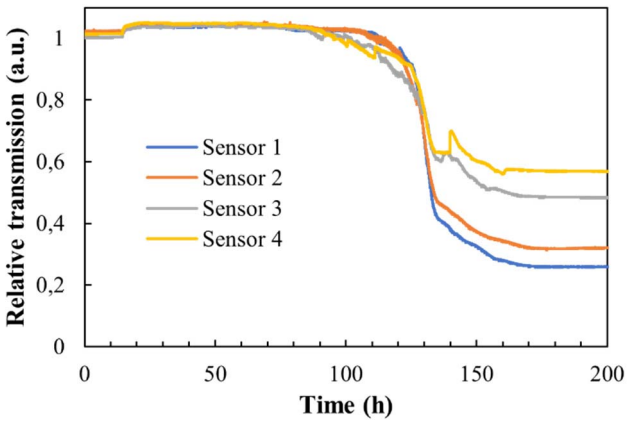

Fig. 13. Results of the test sample coated with epoxy primer.

the rust changes the surface actively under the sensing optical fibers, thus causing variations in the transmitted optical power, i.e., the relative transmitted optical power tends to decrease constantly during the onset of the corrosion process, which can be detected reliably.

More realistic operation of the sensing principle was further demonstrated by the preparation of the same experiment as described above by using a marine-grade epoxy primer (SeaLine) as a protective coating. The latter is designed as a corrosion protective layer for metal surfaces operating in marine environments. Again, two pairs of sensors (two periodic and two random perturbation sensors) were prepared on the same metal sample. Three layers of epoxy primer were applied over the sensing fibers using a spray gun according to the manufacturer's specifications and left to dry fully [see Fig. 12(a)].

The coating thickness was about 35 μm and was obtained through the small uncoated section left on the sample prior to the test and a 3-D laser scanning microscope. This is still substantially thinner than the manufacturer-recommended coating thickness (80–200 μm) to allow accelerated testing.

The test sample with sensors was then inserted into the test chamber and exposed to corrosive vapors after the initial period of 18 h. Relative sensors' transmission started to decrease significantly after 130 h and reached a steady value after 160 h. The steady-state transmission corresponded to about 50% of the initial transmission in the case of the random

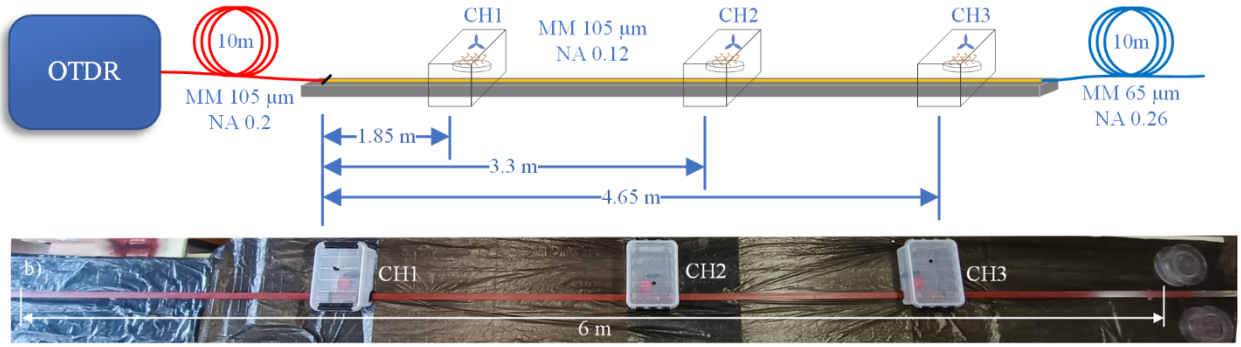

Fig. 14. (a) Test setup using OTDR. (b) Prepared test sample for distributed sensing.

perturbation sensors and 25% in the case of the periodic perturbation sensors, as presented in Fig. 13.

While the sensors with the periodic perturbation structure exhibited higher sensitivity than the sensors with random perturbations, these differences did not appear to be excessive in this configuration, which can likely be attributed to similar Young's modulus of the protective coating and spray filler used to create the periodic perturbations, which limits the creation of the profound periodic sensing fiber's vertical displacement profile.

D. Experimental Investigation of Sensors for Distributed Sensing

The sensors based on periodic stripes and random perturbation sensors fixed with protective coating described in the previous section both exhibited low initial optical losses and can, thus, be mounted over larger surface areas. This provides a possibility for the realization of fully distributed corrosion sensors, which allows for the localization of the corrosion appearance.

To evaluate the possibility for the realization of distributed corrosion sensors, we prepared an experimental setup, which consisted of a longer section of the sensing fiber (AFM105/125/145), which was fixed to a 6 m long and flat steel (S235JR + C) strip using both (periodic and random microbend) sensor designs. In the first design, the fiber was fixed directly to the metal surface using a primer coating. In the second design, the fiber was first fixed to the metal surface using periodic stripes and then coated with a protective primer, as described in Sections II-B and II-C. Commercial marine grade epoxy primer (SeaLine) was used as a protection layer. The sensing fibers were connected individually to a high-resolution optical time domain reflectometer (OTDR) VIAVI MTS6000A with a spatial resolution of 10 cm and rms dynamic range of 12 dB, through 10 m of launch/lead fiber (WF 105/125/140 P, Ceram Optec) with a core diameter of 105 μm and NA of 0.2 (see Fig. 14). Launch fiber was inserted to avoid the event dead zone of the OTDR, which was 0.2 m. The higher NA of the launch/lead fiber provides lower sensitivity to macrobending outside the sensing area and provides the delay required for the OTDR receiver recovery caused by the reflection from the input connector.

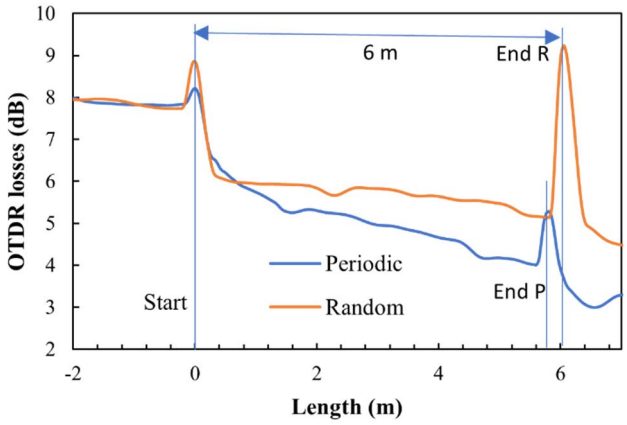

Fig. 15. Initial OTDR traces of periodic and random microbend corrosion sensors before exposure to the corrosive environment.

Since the NA of the delay and the sensing fiber is different, a signal level drop in the OTDR trace at the start position of the sensing fiber is expected.

An additional 10 m of the standard MM fiber with a core diameter of 62.5 μm was also spliced to the end of the sensing fiber, primarily to decrease back reflection at the end of the sensing fiber and prevent the saturation of the detector. To initiate the corrosion process controllably at predetermined test strip locations, we encompassed the test metal strip locally into three miniaturized test corrosion chambers with widths of 25 cm, located at different positions along the sample, as shown in Fig. 14 (the chambers were located 1.85, 3.3, and 4.65 m measured from the beginning of the sensing fiber).

For comparison, both sensor types (periodic and random microbend) were prepared on the same metal sample strip. The periodic microbend sensor was prepared using periodic cutouts within the masking tape, which were cut out using a CO_2 laser. This simplified and accelerated the manufacturing process of the long masking tape significantly. Fixing the fiber using the masking tape also assured that the fiber was pressed firmly to the metal surface over the entire test length before the application of the spray filler. Mounting of the sensor based on the random perturbation principle on the test strip also required temporary fiber fixing onto the observed surface, which was provided by narrow sections of masking tape located about 30 cm apart. After applying the first two layers of the coating,

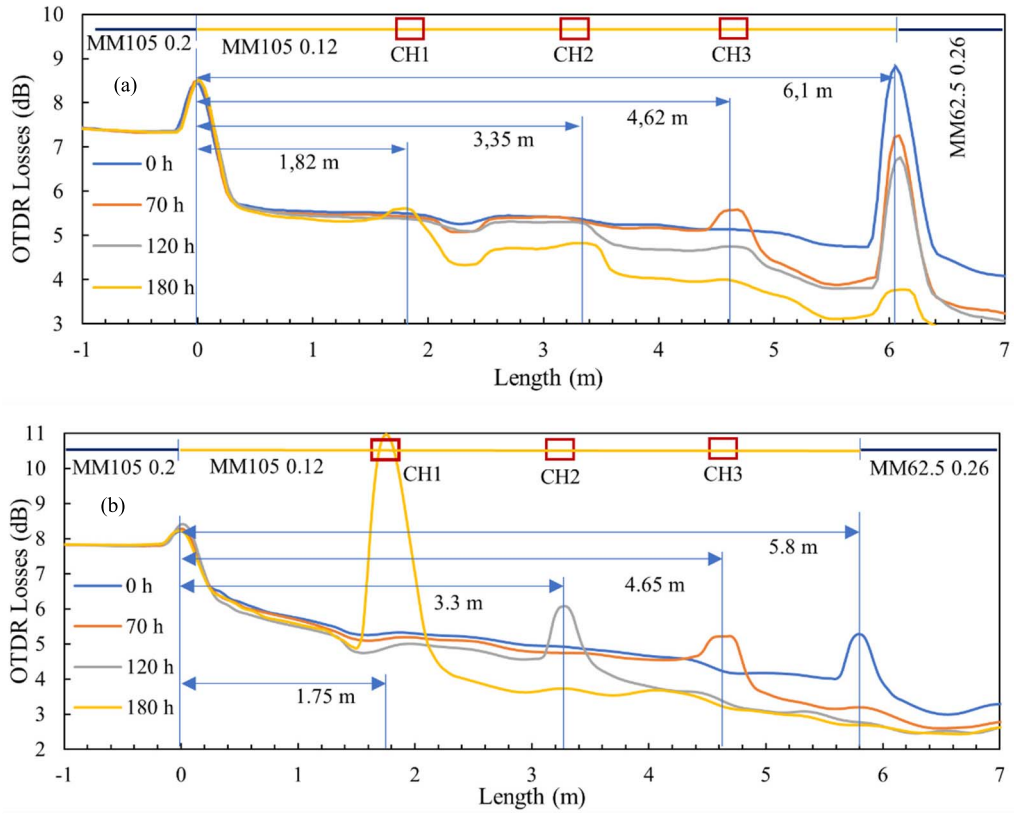

Fig. 16. OTDR traces obtained during the corrosion process on a sensor based on (a) random microbending and (b) periodic microbending. The red squares represent corrosion chamber width and locations.

these masking tape sections were removed, and the final two layers of the epoxy primer were applied over the entire length of the metal test strip (see Fig. 14).

Both sensor types (randomly and periodically perturbated) were connected to the OTDR for initial measurements. Pulsewidth of OTDR was set to 1 ns (spatial resolution of 10 cm, and dynamic range of 12 dB), test range of 50 m, and data acquisition time (averaging) was set to 3 min. The sensor based on periodic perturbations exhibited larger (0.4 dB/m) but overlength uniform initial losses (see Fig. 15). The initial losses of the sensing fiber in the random perturbation configuration appeared to be similar to the lead lead-in fiber losses (0.11 dB/m).

The corrosion process on the test sample was then provoked sequentially by introducing a corrosion atmosphere into the test chambers, starting with the chamber at the most distant location from the OTDR, i.e., in chamber 3 (CH3). Once the sensors began to show the signs of corrosion in a specific chamber, corrosion was provoked within the next closest chamber. The evolution of OTDR traces over time for both sensors is shown in Fig. 16. From all the recorded OTDR traces, the appearance of the corrosion process and its location along the test strip can be recognized unambiguously, as the application of the corrosive solution into the individual chambers created clearly distinguishable events in the OTDR traces at locations that correspond to chamber locations.

The obtained OTDR traces indicate that the periodic perturbation microbend sensors' overall sensitivity is higher than sensors using a random microbend design. In the case of periodic perturbation sensors, a fully corroded section within the chamber caused losses, which exceeded the used OTDR's dynamic range. Thus, the sensing fiber beyond the fully corroded section became undetectable [see Fig. 16(b)]. In contrast, the entire length of the random microbend sensor was visible even at the end of the test [see Fig. 16(a)]. At locations of strong microbending, both sensors generated significant back-reflections, which is a known phenomenon often found in plastic optical fibers [31], [32] but also in silica fibers [33] with large core diameter, low NA, and step-index profile (in our case, we used step-index silica fiber with 105-μm core diameter, 125-μm fiber diameter, and NA of 0.12). Bending of such fiber causes sufficient changes in core refractive index due to bending stress [34], which further cause backscattering and more efficient local coupling of scattered light.

To avoid any other sources of losses that can occur along the fiber during operation of the system (macrobending, connectors, etc.), it is necessary to perform initial measurement after the sensor is installed. All other measurements are then compared to the initial measurement. Alternatively, the sensor can be interconnected with high NA lead fibers, which possess high micro- and macro-bend loss tolerance.

E. Discussion: Comparison of Periodic and Random Microbend Sensor Designs

Sensors based on periodic microbend perturbation require controlled formation of a firm periodic attachment of the sensing fiber onto the observed surface. While there are different possible ways of achieving this, the proposed procedure using masking tape with periodic cutouts and application of a spray filler seems straightforward and efficient, as it allows for controlled and firm periodic bonding of the fiber onto the observed surface, even when the surface has a complex shape. This sensor variant also demonstrated the highest sensitivity to the onset of corrosion events. Furthermore, the periodic microbend perturbation sensor design enables straightforward corrosion sensing in cases of uncoated samples. On the negative side, periodic attachment can cause larger initial optical losses, limiting the operating range of this type of sensor significantly when used in distributed configurations. Some of these limits can be extended by using the OTDR with a larger dynamic range, allowing for observation over longer distances. Photocounting OTDRs might be especially suitable in case when short-range observations are required.

Sensors based on random microbending, on the other hand, require fewer steps in manufacturing and installation. They are intrinsically the simplest in design, e.g., they are essentially composed of a proper sensing fiber attached to the observed surface by a (protective) coating. However, care must be taken when mounting them on more complex/curved surfaces, as the fiber must retain good contact with the surface over the entire length of the sensor (the coating shall not penetrate and form a thin intermediate layer between the fiber and the observed surface). The sensitivity of these sensors is lower in comparison to periodically perturbed sensor designs. However, lower sensitivity does not necessarily lead to a disadvantage in the case of distributed sensing configuration. Limited sensor responses (lower sensitivity), which do not induce excessive optical losses in the fiber, provide more possibilities to monitor larger and/or multiple corrosion events along the sensing fiber. More importantly, initial losses after installation are the lowest in random microbending sensors, which makes this type of sensor a preferred choice for constructing distributed sensors for monitoring larger areas.

Both designs could offer the possibility to evaluate the corrosion quantitatively; however, many parameters, such as corrosion type, metal composition, sensor fixing method, protective coating, and environment, can affect the measurement result. To consider all of those parameters, a more detailed investigation would be required.

IV. Conclusion

This research yielded two different designs of distributed corrosion sensors based on microbend losses capable of detecting corrosion and corrosion location under the protective coatings.

Corrosion-induced microbending of the fiber was achieved either by depression of the sensing fiber against the observed surface or by attaching the sensing fiber periodically to the observed surface. In both cases, the volumetric expansion of the corroding surface material leads to either random or periodic displacements of the sensing fiber from its horizontal axis, which results in optical transmission loss modulation within the sensing fiber.

Several sensors' design variants were investigated systematically, while the proposed sensors were configured and demonstrated successfully in a single point and distributed configurations. The proposed sensor designs can also be used on bare metal surfaces or relatively unobtrusively applied underneath corrosion-protective coatings. The investigated sensors are intrinsically simple; their design and production are essentially reduced to a proper fiber selection and mounting onto the observed surface. The latter can be accomplished in different ways, including direct attachment of the sensing fiber to the monitored surface, even by applying an anti-corrosion protective coating that is otherwise utilized for the structure's corrosion protection. Periodic mounting of the fiber to the surface can also be made, which improves sensitivity and simplifies the mounting procedure but adds to sensor complexity and increases the initial sensor losses. The latter might affect the sensor' range and the ability to address multiple events in the case of distributed sensor configurations. On the other hand, a periodic attachment structure is straightforwardly applicable in noncoated or soft-coated monitored surface cases. Both configurations require a proper selection of sensing optical fibers, which shall exhibit sufficient microbend sensitivity. While standard telecom fibers proved to be inadequately sensitive for straightforward sensor realization, among commercially available fibers, low NA, large-core MM fibers used for high-power laser pump combiner production provided all the characteristics required for successful sensor design and sensor demonstration. By application of these fibers, a few centimeter long corrosion affected sections provided sufficient loss modulation (within the several decibel range) that can easily be detected by an appropriate optical setup.

In the case of distributed sensor configurations, the spatial resolution of the corrosion event localization is limited mainly by the resolution of the OTDR and was about 10 cm in the currently investigated experimental configuration (using high-resolution, cost-efficient OTDR intended for avionics network testing and similar short-range applications). By utilizing short-range photocounting OTDRs, this resolution and dynamic range could be improved further. It should also be stressed that this research was limited to commercially available optical fibers. Customization of a sensing fiber, i.e., optimization/adjustment of its NA, core size, outer fiber diameter, and fiber primary coating material and coating diameter, which all affect fiber microbend performance profoundly, can provide an opportunity for further optimization and tailoring of microbend corrosion sensors to specific applications.

Simplicity and the possibility for straightforward realization of the described sensors are probably two of the main advantages of the presented concept. Furthermore, unlike other known optical fiber corrosion sensor solutions, the presented sensors require very low-complexity signal interrogation, i.e., intensity interrogation in cases of single-point sensors and use of standard telecom or nearly standard OTDR in a distributed

configuration, which provides possibilities for the design of economically viable and attractive solutions.

ACKNOWLEDGMENT

Authorship contribution statement: Matej Njegovec: methodology, conceptualization, investigation, validation, software, writing—original draft, writing—review and editing, and visualization. Vedran Budinski: formal analysis, writing—review, and editing. Boris Macuh: investigation, software, resources, writing—review, and editing. Denis Đonlagić: conceptualization, supervision, project administration, funding acquisition, writing—review, and editing.

REFERENCES

[1] L. Qin, H. Ren, B. Dong, and F. Xing, "Development of technique capable of identifying different corrosion stages in reinforced concrete," *Appl. Acoust.*, vol. 94, pp. 53–56, Jul. 2015, doi: 10.1016/j.apacoust.2015.01.013.

[2] E. Yahaghi, A. Movafeghi, B. Rokrok, and M. Mirzapour, "Defects detection of digital radiographic images of aircraft structure materials via geometric locally adaptive sharpening," *Res. Nondestruct. Eval.*, vol. 31, no. 2, pp. 107–115, Mar. 2020, doi: 10.1080/09349847.2019.1634226.

[3] Y. Shi, C. Zhang, R. Li, M. Cai, and G. Jia, "Theory and application of magnetic flux leakage pipeline detection," *Sensors*, vol. 15, no. 12, pp. 31036–31055, 2015, doi: 10.3390/s151229845.

[4] Y. Zhang and J. Moloney, "Electrochemical corrosion rate measurement under iron sulfide deposit," *Corrosion*, vol. 72, no. 5, pp. 704–715, May 2016, doi: 10.5006/1763.

[5] J. Goellner, A. Burkert, A. Heyn, E. Boese, O. Ezers'ka, and J. Hickling, "State-of-the-art of corrosion testing by using electrochemical noise measurements," *Mater. Sci.*, vol. 37, no. 3, pp. 509–519, 2001, doi: 10.1023/A:1013222525386.

[6] R. Rodrigues, S. Gaboreau, J. Gance, I. Ignatiadis, and S. Betelu, "Reinforced concrete structures: A review of corrosion mechanisms and advances in electrical methods for corrosion monitoring," *Construct. Building Mater.*, vol. 269, Feb. 2021, Art. no. 121240, doi: 10.1016/j.conbuildmat.2020.121240.

[7] C. Du, Q. Tang, J. Zhou, X. Guo, T. Yu, and X. Wang, "Fiber optic sensors based on photoacoustic effect for rebar corrosion measurement," *IEEE Trans. Instrum. Meas.*, vol. 68, no. 11, pp. 4559–4565, Nov. 2019, doi: 10.1109/TIM.2018.2890318.

[8] H. P. Alves, J. F. Nascimento, E. Fontana, I. J. S. Coelho, and J. F. Martins-Filho, "Transition layer and surface roughness effects on the response of metal-based fiber-optic corrosion sensors," *J. Lightw. Technol.*, vol. 36, no. 13, pp. 2597–2605, Jul. 1, 2018, doi: 10.1109/JLT.2018.2817517.

[9] D. Luo, Y. Li, T. Lu, K. Lim, and H. Ahmad, "Tapered polymer optical fiber sensors for monitoring the steel bar corrosion," *IEEE Trans. Instrum. Meas.*, vol. 70, 2021, Art. no. 6008909, doi: 10.1109/TIM.2021.3097405.

[10] M. R. Islam, M. Bagherifaez, M. M. Ali, H. K. Chai, K.-S. Lim, and H. Ahmad, "Tilted fiber Bragg grating sensors for reinforcement corrosion measurement in marine concrete structure," *IEEE Trans. Instrum. Meas.*, vol. 64, no. 12, pp. 3510–3516, Dec. 2015, doi: 10.1109/TIM.2015.2459511.

[11] Y. Chen, F. Tang, Y. Tang, M. J. O'Keefe, and G. Chen, "Mechanism and sensitivity of Fe-C coated long period fiber grating sensors for steel corrosion monitoring of RC structures," *Corrosion Sci.*, vol. 127, pp. 70–81, Oct. 2017, doi: 10.1016/j.corsci.2017.08.021.

[12] W. Hu, H. Cai, M. Yang, X. Tong, C. Zhou, and W. Chen, "Fe–C-coated fibre Bragg grating sensor for steel corrosion monitoring," *Corrosion Sci.*, vol. 53, no. 5, pp. 1933–1938, May 2011, doi: 10.1016/j.corsci.2011.02.012.

[13] W. Hu *et al.*, "Optical fiber polarizer with Fe–C film for corrosion monitoring," *IEEE Sensors J.*, vol. 17, no. 21, pp. 6904–6910, Nov. 2017, doi: 10.1109/JSEN.2017.2743245.

[14] D. C. Sweeney, A. M. Schrell, and C. M. Petrie, "Pressure-driven fiber-optic sensor for online corrosion monitoring," *IEEE Trans. Instrum. Meas.*, vol. 70, pp. 1–10, 2021, doi: 10.1109/TIM.2021.3089231.

[15] N. Zhang, W. Chen, X. Zheng, W. Hu, and M. Gao, "Optical sensor for steel corrosion monitoring based on etched fiber Bragg grating sputtered with iron film," *IEEE Sensors J.*, vol. 15, no. 6, pp. 3551–3556, Jun. 2015, doi: 10.1109/JSEN.2015.2393559.

[16] S. Dong, Y. Liao, Q. Tian, Y. Luo, Z. Qiu, and S. Song, "Optical and electrochemical measurements for optical fibre corrosion sensing techniques," *Corrosion Sci.*, vol. 48, no. 7, pp. 1746–1756, Jul. 2006, doi: 10.1016/j.corsci.2005.05.025.

[17] S. Almahmoud, O. Shiryayev, N. Vandati, P. Rostron, and J. Lynch, "Feasibility of magnetic fiber-optic based corrosion sensor," *Proc. SPIE*, vol. 2017, vol. 10168, Apr. 2017, Art. no. 101681M, doi: 10.1117/12.2260882.

[18] M. R. A. Hassan, M. H. A. Bakar, K. Dambul, and F. R. M. Adikan, "Optical-based sensors for monitoring corrosion of reinforcement rebar via an etched cladding Bragg grating," *Sensors*, vol. 12, no. 1, pp. 15820–15826, 2012, doi: 10.3390/s121115820.

[19] O. Almubaied, H. K. Chai, M. R. Islam, K.-S. Lim, and C. G. Tan, "Monitoring corrosion process of reinforced concrete structure using FBG strain sensor," *IEEE Trans. Instrum. Meas.*, vol. 66, no. 8, pp. 2148–2155, Aug. 2017, doi: 10.1109/TIM.2017.2676218.

[20] W. Li, S. C. M. Ho, M. Luo, Q. Huynh, and G. Song, "Fiber optic macro-bend based sensor for detection of metal loss," *Smart Mater. Struct.*, vol. 26, no. 4, Apr. 2017, Art. no. 045002, doi: 10.1088/1361-665X/aa5d5d.

[21] H. Cao, Y. Hao, Z. Zhang, J. Wei, and L. Yang, "System and method of quasi-distributed fiber Bragg gratings monitoring brittle fracture process of composite insulators," *IEEE Trans. Instrum. Meas.*, vol. 70, pp. 1–10, 2021, doi: 10.1109/TIM.2021.3096876.

[22] L. Fan, Y. Bao, and G. Chen, "Feasibility of distributed fiber optic sensor for corrosion monitoring of steel bars in reinforced concrete," *Sensors*, vol. 18, no. 11, p. 3722, Nov. 2018, doi: 10.3390/s18113722.

[23] L. Fan, Y. Bao, W. Meng, and G. Chen, "*In-situ* monitoring of corrosion-induced expansion and mass loss of steel bar in steel fiber reinforced concrete using a distributed fiber optic sensor," *Compos. B, Eng.*, vol. 165, pp. 679–689, May 2019, doi: 10.1016/j.compositesb.2019.02.051.

[24] J. Li, Y. Zhao, and J. Wang, "A spiral distributed monitoring method for steel rebar corrosion," *Micromachines*, vol. 12, no. 12, p. 1451, Nov. 2021, doi: 10.3390/mi12121451.

[25] X. Tan, L. Fan, Y. Huang, and Y. Bao, "Detection, visualization, quantification, and warning of pipe corrosion using distributed fiber optic sensors," *Autom. Construct.*, vol. 132, Dec. 2021, Art. no. 103953, doi: 10.1016/j.autcon.2021.103953.

[26] L. Ren, T. Jiang, Z.-G. Jia, D.-S. Li, C.-L. Yuan, and H.-N. Li, "Pipeline corrosion and leakage monitoring based on the distributed optical fiber sensing technology," *Measurement*, vol. 122, pp. 57–65, Jul. 2018, doi: 10.1016/j.measurement.2018.03.018.

[27] D. Marcuse, "Coupled mode theory of round optical fibers," *Bell System Tech. J.*, vol. 52, no. 6, pp. 817–842, Jul. 1973, doi: 10.1002/j.1538-7305.1973.tb01992.x.

[28] N. Lagakos and J. Bucaro, "Fiber optic microbend sensor," *Opt. Lett.*, vol. 27, no. 1, pp. 19–24, 1988, doi: 10.1364/AO.26.002171.

[29] R. D. Desiati, E. Sugiarti, and K. Z. Thosin, "Effect of cloric acid concentration on corrosion behavior of Ni/Cr coated on carbon steel," *Metall. Adv. Mater. Tech. Sust. Develop.*, vol. 1964, May 2018, Art. no. 020018, doi: 10.1063/1.5038300.

[30] R. Fan, W. Zhang, Y. Wang, D. Chen, and Y. Zhang, "Metal material resistant to hydrochloric acid corrosion," *J. Phys., Conf. Ser.*, vol. 1732, no. 1, Jan. 2021, Art. no. 012134, doi: 10.1088/1742-6596/1732/1/012134.

[31] I. R. Husdi, K. Nakamura, and S. Ueha, "Sensing characteristics of plastic optical fibres measured by optical time-domain reflectometry," *Meas. Sci. Technol.*, vol. 15, no. 8, pp. 1553–1559, Aug. 2004, doi: 10.1088/0957-0233/15/8/022.

[32] T. Fukumoto *et al.*, "A POF-based distributed strain sensor for detecting deformation of wooden structures," *Proc. SPIE*, vol. 7004, May 2008, Art. no. 700469, doi: 10.1117/12.785751.

[33] P. Xu *et al.*, "Distributed refractive index sensing based on bending-induced multimodal interference and Rayleigh backscattering spectrum," *Opt. Exp.*, vol. 29, no. 14, pp. 21530–21538, Jul. 2021, doi: 10.1364/OE.430637.

[34] T. Sugita, "Optical time-domain reflectometry of bent plastic optical fibers," *Appl. Opt.*, vol. 40, no. 6, pp. 897–905, Feb. 2001, doi: 10.1364/AO.40.000897.

Matej Njegovec received the B.S. degree from the Faculty of Electrical Engineering and Computer Science, University of Maribor, Maribor, Slovenia, in 2008, and the Ph.D. degree in electrical engineering from the University of Maribor, in 2013.

He is an Assistant Professor at the University of Maribor. He has excellent background in analog and RF circuit design, semiconductor light sources, optoelectronic components, modulation techniques, signal-processing of modulated light signals, and general signal integration techniques related to optical sensors. His biggest motive is to find innovative and cost-efficient solutions for fiber-optic sensors that would allow for the introduction of fiber-sensor technology into a broader range of practical applications. His main research interests include fiber optic sensors, optical sensor interrogation techniques, and the design of optoelectronic systems.

Vedran Budinski received the B.S. and Ph.D. degrees from the Faculty of Electrical Engineering and Computer Science, University of Maribor, Maribor, Slovenia, in 2012 and 2017, respectively.

Since 2012, he has been working as a Researcher with the Laboratory for Electro-Optical and Sensor Systems, University of Maribor. His research interests include fiber optic sensors for measuring twist/rotation, fiber optic microfluidic sensors, and design of miniature microstructures on the tip of the optical fiber, employing various micromachining techniques for detecting various physical and chemical parameters.

Boris Macuh received the B.S. degree from the Faculty of Electrical Engineering and Computer Science, University of Maribor, Maribor, Slovenia, in 2010.

He is currently a Technical Assistant with the Faculty of Electrical Engineering and Computer Science, University of Maribor. He has more than ten years of researching experiences in field of sensors and measurements, 3-D mechanical modeling, electronic circuit design, and computer numeric control (CNC) operations.

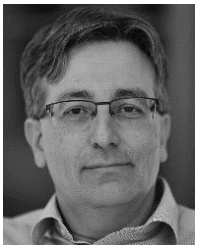

Denis Đonlagić (Member, IEEE) received the dual Ph.D. degrees from the University of Ljubljana, Ljubljana, Slovenia, in 1998, and University of Strathclyde, Glasgow, U.K., in 2000, respectively.

He is a Full Professor at the University of Maribor, Maribor, Slovenia. He has a broad background in the fields of photonics systems, opto-electronics systems, optical fibers, and microoptoelectromechanical system (MOEMS). In particular, he has research and development experience in the fields of optical fiber sensors, optical fibers, and opto-electronics system design. His focus is in finding new scientific paradigms and technology concepts, while bringing them into practical applications.

Dr. Đonlagić is a member of editorial board of the JOURNAL OF LIGHTWAVE TECHNOLOGY.